



# On the features of cooperative mobility in the amorphous phase of ferroelectric polymers

V. V. Kochervinskii<sup>1</sup> · I. A. Malyshkina<sup>2</sup> · M. A. Gradova<sup>3</sup> · N. V. Kozlova<sup>1</sup> · N. A. Shmakova<sup>1,4</sup> · M. I. Buzin<sup>5</sup> · A. A. Korlyukov<sup>5</sup> · S. A. Bedin<sup>6</sup>

Received: 1 November 2018 / Revised: 30 December 2018 / Accepted: 15 January 2019 / Published online: 9 February 2019  
© Springer-Verlag GmbH Germany, part of Springer Nature 2019

## Abstract

Ferroelectric poly(vinylidene fluoride–hexafluoropropylene) films were prepared by low-temperature crystallization from the acetone and ethyl acetate solutions. Crystalline modifications of the obtained films were different (mixture of  $\beta$ - and  $\gamma$ -phases in case of acetone and predominantly  $\alpha$ -phase in case of ethyl acetate). The dielectric spectroscopy studies showed that the relaxation strength of the main relaxation above the glass transition temperature (associated with the cooperative mobility in the amorphous phase) unusually increases with increasing temperature. Thermodynamic relationships suggest that this effect may be explained by assuming that there is a certain long-range order in the amorphous phase. This order may be due to the presence of the local field near the polar planes of the crystals, which form ferroelectric domains.

**Keywords** Ferroelectric polymers · Crystalline polymers · PVDF · Crystallization · Dielectric relaxation

## Introduction

Ferroelectric polymers have attracted considerable attention of researchers due to their possible applications in various fields of technology [1–3]. Among them, poly(vinylidene fluoride) (PVDF) and its copolymers is the most prominent. At high-voltage polarization, they exhibit piezo- and pyroelectricity that allows them to be used in various technical devices. Despite the fact that piezoelectric constants in these polymers

are more than an order of magnitude lower than in classical inorganic ceramics, in some cases, the preference is given to polymers because of their specific properties, for example, high-impact viscosity and low mechanical Q-factor. The latter provides a wide dynamic range, which allows creating polymer-based shockwave sensors [4]. Another important property of the materials under study is their low acoustic impedance close to that in water, which allows their application in hydroacoustics [5]. High thermoplasticity of the polymers under consideration enables to fabricate active devices with a large surface area using extrusion techniques. All these features create possibilities for the development of alternative sources that convert sea (river) energy into electrical energy [6]. All of the above properties enable such materials to be used on ships for preventing bio-corrosion [7]. After directional structural modification of the polymers under consideration, due to their large electrocaloric effect, miniature micro-coolers can be developed [8]. Due to high breakdown voltage, the polymers can also be used in effective capacitive energy storage devices [9].

All of these applications are based on the ferroelectric nature of the considered polymers, and therefore the investigations of the details of the domain structure formation in them are of special interest. The crystalline polymers under consideration are structurally different from the ferroelectric inorganic crystals and ceramics. They generally consist of at

✉ V. V. Kochervinskii  
kochval@mail.ru

<sup>1</sup> State Research Center of the Russian Federation Karpov Institute of Physical Chemistry, Vorontsovo Pole 10, 103064 Moscow, Russia

<sup>2</sup> Faculty of Physics, M.V. Lomonosov Moscow State University, Leninskie Gory 1 bld 2, 119991 Moscow, Russia

<sup>3</sup> Semenov Institute of Chemical Physics, Kosygina Str. 4 bld 1, 119991 Moscow, Russia

<sup>4</sup> Enikolopov Institute of Synthetic Polymeric Materials, Profsoyuznaya Str. 70, 117393 Moscow, Russia

<sup>5</sup> Nesmeyanov Institute of Organoelement Compounds, Vavilova str. 28, 119991 Moscow, Russia

<sup>6</sup> Moscow State Pedagogical University, M. Pirogovskaya Str. 1/1, 119991 Moscow, Russia

minimum two phases—crystalline and amorphous—in approximately equal fractions. This means that the materials have structural heterogeneity. If the polymer is above the glass transition temperature ( $\sim -40$  °C), the chains of the amorphous phase are in a liquid-like state, since they participate in cooperative motions with short relaxation times [10]. This means that along with structural heterogeneity, there is also a dynamic heterogeneity in such polymers.

Among numerous VDF copolymers, attention should be paid to VDF copolymers with hexafluoropropylene (HFP), since they achieved high electrical breakdown fields that allows employing them as high-energy-density capacitors [9]. Since the noted dynamic heterogeneity may affect the above-mentioned breakdown fields, we studied in detail the molecular mobility in this class of fluoropolymers by broadband dielectric spectroscopy. By the example of this copolymer, we also checked the possibility of obtaining various polymorphic modifications at the crystallization from a solution. We demonstrate that this could be achieved by using solutions in specific solvents. It is observed that the relaxation strength and the activation barrier of the micro-Brownian mobility in the amorphous phase are noticeably lower for the films crystallized in the non-polar  $\alpha$ -phase. The analysis showed that this is mainly due to the changes of the effective dipole moment of the kinetic units. An unusual increase in the relaxation strength with increasing temperature should be attributed, according to thermodynamic relations, to the formation of a certain long-range order in the regions of the amorphous phase adjacent to the polar crystals.

## Materials and methods

The films of VDF/HFP 93/7 copolymer were prepared by a crystallization from the acetone (film I) and ethyl acetate (film II) solutions at a room temperature. To study the electrical characteristics of copolymer films, 50-nm-thick Au electrodes were deposited on the films by thermal sputtering.

Broadband dielectric spectroscopy measurements were performed on a Novocontrol Concept 40 broadband dielectric spectrometer with temperature control in isothermal regime. The frequency range was from  $10^{-1}$  to  $10^7$  Hz, and the temperature was varied from  $-100$  to  $20$  °C.

IR spectra were recorded with a Bruker Equinox 55s (with Fourier transform) spectrometer. Shooting was performed in transmission and attenuated total reflection ATR (ZnSe crystal) regimes; the latter was used to probe  $0.5\text{--}2$   $\mu\text{m}$  thick surface layer of polymer.

Differential scanning calorimetry (DSC) analysis was conducted on DSC-822e (Mettler-Toledo, Switzerland) at a heating/cooling rate  $10$  °C/min in argon atmosphere.

The powder X-ray diffraction (XRD) measurements were performed with a Bruker D8 Advance diffractometer (Vario

$K\alpha_1$  geometry) equipped with a  $K\alpha_1$  Ge(111) focusing monochromator and a LynxEye 1D position-sensitive detector in transmission mode. The scanning range was from  $7$  to  $60^\circ$ .

## Experimental results and discussion

The main objective of this work was to clarify the differences in the conformational structure and the micro-Brownian cooperative dynamics of the chains in the amorphous phase in two different samples above the glass transition point ( $\alpha_a$ -relaxation). These samples, as will be shown below, crystallize in different polymorphic modifications, but it is completely unclear how this will affect the microstructure of the amorphous phase and, accordingly, the character of the noted dynamics. The analysis was carried out using the data of temperature-frequency dependences of the components of the complex dielectric constant, which are shown in Fig. 1 for one of the studied samples (II). The loss spectra reveal two clearly resolved relaxation peaks contributed by the  $\alpha_a$ -relaxation and  $\alpha_c$ -relaxation. As follows from the same dependences for sample I (Fig. 2), only one region of molecular mobility is seen ( $\alpha_a$ -relaxation), which overlaps with the onset of the high-temperature space charge relaxation process in the low-frequency region. In such conditions, it was important to find the correct way to obtain the parameters of the  $\alpha_a$ -process. For

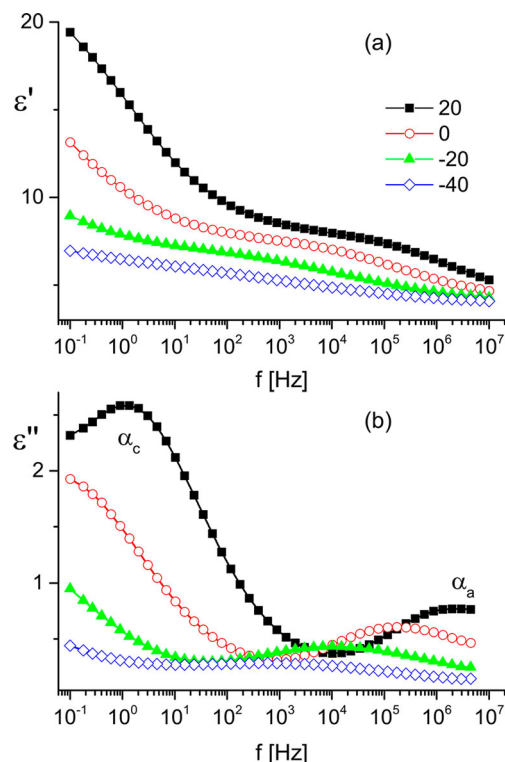


**Fig. 1** Frequency dependences of the real  $\epsilon'$  (a) and imaginary  $\epsilon''$  (b) components of the complex dielectric permittivity for sample II at different temperatures indicated on the plot

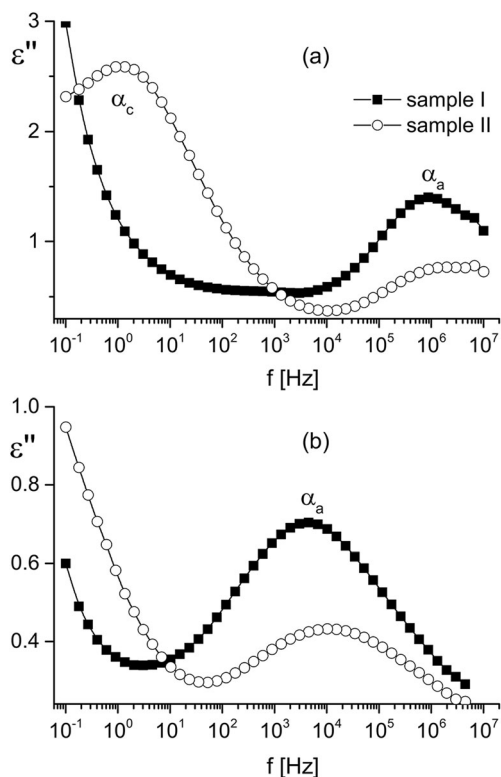


**Fig. 2** Frequency dependences of the dielectric loss  $\epsilon''$  for samples I and II at 20 (a) and  $-20$  °C (b)

this, we have analyzed the frequency dependences of the components of the complex dielectric constant at temperatures near and slightly higher than the glass transition temperature, where the contribution from high-temperature relaxation processes can be neglected.

The dielectric spectroscopy data in the region of the  $\alpha_a$ -relaxation were fitted by the Havriliak-Negami function:

$$\epsilon^*(\omega) = \epsilon_\infty + \frac{\Delta\epsilon}{(1 + (i\omega\tau_\alpha)^b)^c}, \quad (1)$$

where  $\Delta\epsilon = \epsilon_s - \epsilon_\infty$  is the dielectric relaxation strength ( $\epsilon_s$  and  $\epsilon_\infty$  are low- and high-frequency limits of the dielectric function),  $\tau_\alpha$  is the most probable relaxation time, and  $b$  and  $c$  ( $0 < b, bc \leq 1$ ) are the shape parameters describing symmetric and asymmetric broadening of the complex dielectric function.

It is seen from the presentation of experimental data on the complex plane (Fig. 3) that the absolute values of the static dielectric permittivity  $\epsilon_s$  and their temperature dependencies for the samples are noticeably different.

Figure 4 shows the temperature dependences of most probable reorientation frequencies  $f_\alpha = \frac{1}{2\pi\tau_\alpha}$  of polymer segments in Arrhenius coordinates. For both samples, the curved character of the dependences indicates that the micro-Brownian cooperative dynamics of the amorphous segments is registered above the glass transition temperature

[10]. Such dependences obey the Vogel-Thamman-Fulcher (VTF) law [11]:

$$f_\alpha = f_{0\alpha} \exp\left(-\frac{B}{T-T_0}\right), \quad (2)$$

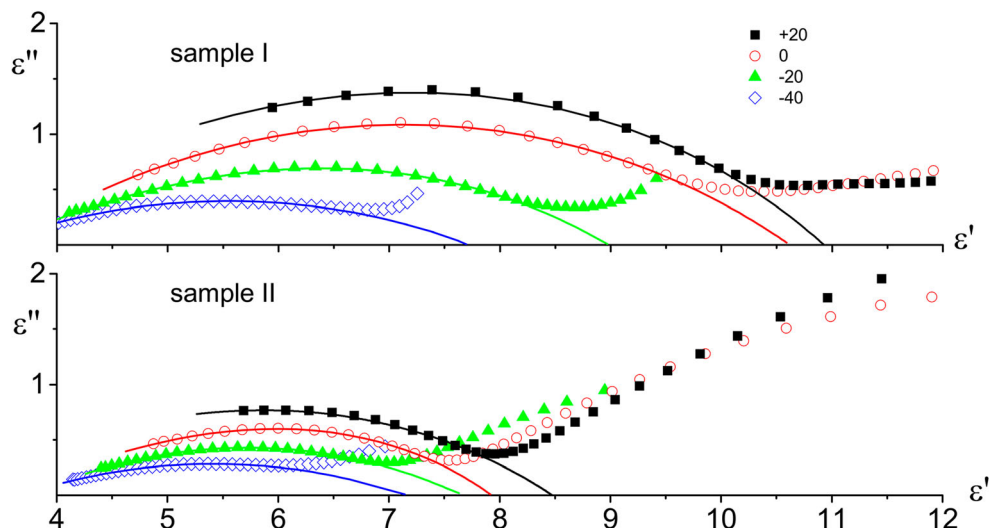
where  $T_0$  is the Vogel temperature, which is usually nearly  $50$  °C lower than the glass transition temperature, as estimated by DSC, and  $B$  characterizes the activation barrier for the mobility.

These and other parameters, obtained from the fits, are given in Table 1 for both samples. It follows from the table that the activation barrier in sample I turns out to be a quarter higher than that in sample II. Figure 5 demonstrates the temperature dependences of the dielectric relaxation strength  $\Delta\epsilon$  of the  $\alpha_a$ -relaxation, which, as can be seen, differ significantly for both samples. Thus, the data presented above indicate significant differences in the cooperative dynamics of the chains in the amorphous phase of the samples under consideration. The task of the further analysis was to clarify the causes of the noted phenomenon.

We can expect that the studied samples differ in structure due to the polymorphism at the PVDF crystallization [1, 2] and to the specific effect of the solvents on the final structure of the polymers [1, 2, 10]. In order to confirm this hypothesis, the crystalline properties of the films were characterized with XRD and IR spectroscopy. As shown in Fig. 6, the copolymer II crystallizes predominantly in the non-polar  $\alpha$ -phase. The smallest-angle peak observed at  $2\theta = 16.2^\circ$  (halo) is associated with the presence of the metastable paraelectric phase. The appearance of this phase is due to the low crystallization temperature, since it was also found in VDF copolymers with tetrafluoroethylene (TFE) under the same crystallization conditions [12]. The comparison of the data with our previous paper [12] shows that the positions of the peaks assigned to the paraelectric phase and to the  $\alpha$ -phase are shifted to the smaller angles in the studied copolymer. This means that the lattice both in the crystalline and in the paraelectric phases is less densely packed than in pure PVDF [1, 2, 10]. We believe that the reason for this is the presence of HFP groups which have large steric hindrances.

Structural differences in the films were studied in detail by IR spectroscopy, which provide conformation-sensitive IR bands [1, 2]. The bands typical for different polymorph modifications of the PVDF are marked on the curves in Fig. 7. It can be seen that sample I crystallizes in the mixture of  $\beta$ - and  $\gamma$ -phases, while sample II predominantly in the  $\alpha$ -phase. Using this method, the presence of certain isomers in the chain is recorded, irrespectively of the phase (crystalline or amorphous) where the macromolecules are located. This leads to the important conclusion that if the crystal is formed, for example, in the  $\alpha$ -phase with  $TGTG^-$  chain conformation [1, 2,

**Fig. 3** Cole-Cole diagrams  $\varepsilon''(\varepsilon')$  for samples I and II at several temperatures indicated on the plot. Lines are fits to Eq. (1)



[10], then the chains in the amorphous phase will also have this conformation.

The crystalline properties of the samples were also characterized by DSC. As shown in Fig. 8, the melting temperatures of the films differ insignificantly, but the heat effect for sample II is higher than that for sample I. Correspondingly, the crystallinity of the latter is reduced (Table 1), but the low-temperature endotherm is more pronounced.

Comparison of the data in Figs. 1, 2, and 3 shows that the crystallization of the copolymer in the  $\alpha$ -phase is accompanied by the appearance of a new (low-frequency)  $\alpha_a$ -relaxation. This relaxation is related to the mobility in the crystalline region of the  $\alpha$ -phase [13–16], and the most supported mechanism is a diffusion of the longitudinal component of the dipole moment of the monomeric PVDF unit in the  $TGTG^-$  conformation along the  $c$ -axis [17].

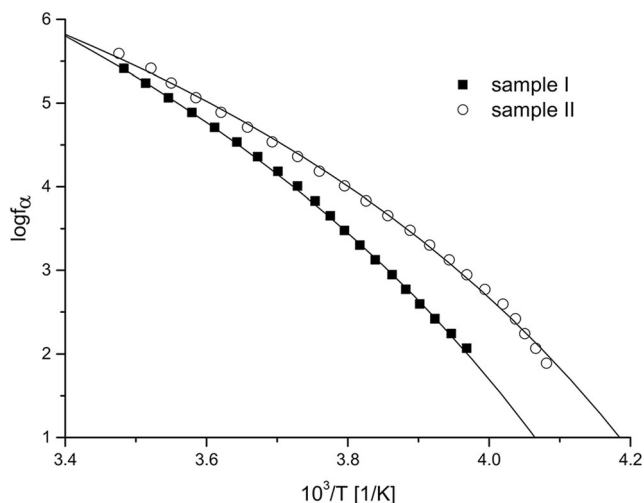


**Fig. 4** Temperature dependences of the reorientation frequencies in Arrhenius coordinates for samples I and II. Lines are fits to Eq. (2)

The values of the fragility  $m$  [18]

$$m = \left. \frac{d(\log \tau_{\alpha})}{d\left(\frac{T_g}{T}\right)} \right|_{T=T_g} \quad (3)$$

are displayed in Table 1. The comparison of the parameters of cooperative dynamics ( $\alpha_a$ -process) in the samples under consideration shows that although the values of the fragility  $m$  are close to each other, the magnitude of the activation barrier (parameter  $B$ ) differs significantly. It turns out to be higher in sample I, where, according to our data, the parts of the chains in the amorphous phase have planar zigzag or  $T_3GT_3G^-$  conformations. This circumstance leads to a higher glass transition temperature (Table 1). Another feature of the polymers under consideration is that their micro-Brownian dynamics ( $\alpha_a$ -process) is characterized, as seen, by the high activation barrier. It is interesting to compare this parameter with the data for similarly crystallized VDF/TFE copolymers, where the fraction of VDF is approximately the same as in the studied copolymer [12]. It turned out that in the VDF/TFE copolymer, the activation barrier is about two times lower. The most probable reason for this is the strong steric hindrance of the kinetic units at micro-Brownian mobility of the chains above the glass transition temperature because of the presence of HFP groups. At the same time, the high barrier for the reorientation of the segments in the amorphous phase will reduce the mobility of the impurity and injected carriers in the amorphous phase of the copolymer. Probably, this circumstance is the cause of very high electric breakdown fields in this class of polymers [9].

In this paper, we will focus on the analysis of the temperature behavior of the dielectric relaxation strength  $\Delta\varepsilon$  of the  $\alpha_a$ -relaxation, which, as noted, is related to the cooperative mobility of the chains in the amorphous phase above the glass

**Table 1** Parameters of the  $\alpha_a$ -relaxation and characteristics of the thermal effects in VDF/HFP samples I and II. Here,  $T_g$  is the glass transition temperature,  $m$  is the fragility,  $T_m$  is the melting temperature,  $\Delta H$  is the enthalpy, and  $\chi_{\text{dsc}}$  is the crystallinity

| Sample | B              | $T_g$ , K | Fragility, $m$ | $\frac{\partial \varepsilon_s}{\partial T}$ | $\Delta H_{\text{lt}}$ , J/g | $T_m$ , °C | $\Delta H_m$ , J/g | $\chi_{\text{dsc}}$ |
|--------|----------------|-----------|----------------|---|------------------------------|------------|--------------------|---------------------|
| I      | $1307 \pm 122$ | 231       | 82             | 0.072                                       | 0.9                          | 122.2      | 26.6               | 0.25                |
| II     | $1041 \pm 137$ | 225       | 80             | 0.017                                       | 0.4                          | 119.2      | 33.8               | 0.32                |

transition temperature. It is usually estimated using the general relationship [19]

$$\Delta\varepsilon = \varepsilon_s - n^2 = \frac{3\varepsilon_s}{2\varepsilon + n^2} \frac{n^2 + 2}{3} \frac{4\pi N}{V} \frac{\mu_0^2 g}{3kT}, \quad (4)$$

where the high-frequency permittivity  $\varepsilon_\infty \approx n^2$ , and  $N$  is the number of kinetic units (dipoles) with a “vacuum” dipole moment  $\mu_0$  in the volume  $V$ .

For a condensed state, the correlation factor  $g$  in the Fuoss-Kirkwood representation

$$g = 1 + Z\langle \cos \gamma \rangle \quad (5)$$

takes into account the nearest environment of  $Z$  neighboring molecules characterized by an average angle  $\gamma$ . As follows from Eq. (4), the temperature increase should lead to the decrease in  $\Delta\varepsilon$ , which is usually the case for most polymer dielectrics [20]. Equation (4) is valid for polar media (including polymers) under the assumption that the local field is described by the Onsager equation.

In the crystalline polymers, the concentration of the mobile polar groups decreases due to the volume occupied by the crystals. Since the crystallinity  $\chi_{\text{dsc}}$  is somewhat higher in sample II than in sample I (see Table 1), then there must be

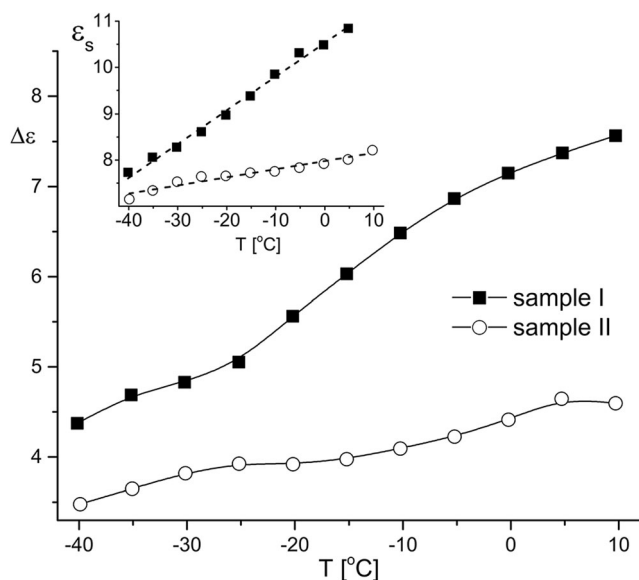


**Fig. 5** Temperature dependences of the dielectric relaxation strength  $\Delta\varepsilon$  for the  $\alpha_a$ -relaxation for samples I and II; in the insert—temperature dependences of the static dielectric constant  $\varepsilon_s$  for the  $\alpha_a$ -relaxation for samples I and II

a slight decrease of  $\Delta\varepsilon$  for the  $\alpha_a$ -relaxation. As follows from Fig. 5, it is really observed but, in our opinion, this reason is not the main one. Indeed, the difference in the curves in Fig. 5 turns out to be temperature-dependent, which cannot be explained only by the change in the concentration of the kinetic polar segments of the amorphous phase. As noted above, the chains have different conformations not only in crystals but also in the amorphous phase, i.e., the chains in the amorphous phase are predominantly in the  $T_3GT_3G^-$  ( $\gamma$ -phase) and planar zigzag ( $\beta$ -phase) conformations in sample I, and in the  $TGTG^-$  conformation in sample II [1, 2, 10]. This all means that the dipole moments  $\mu_0$  can also differ for the chains in the amorphous phase of samples I and II, which leads to the change in the relaxation strength of the  $\alpha_a$ -relaxation.

Under the conditions of polymorphism in ferroelectric PVDF [1, 2] and the presence of the crystalline phase, the dielectric properties of the amorphous phase cannot be described by the Onsager internal field. In such a heterogeneous medium as a crystalline ferroelectric polymer, it is necessary to take into account other factors that can contribute into the local field  $E_L$ . From general considerations, we can write [21]

$$E_L = E_C + \sum E_D, \quad (6)$$

where  $E_C$  is the external field. The additional components of the local field

$$\sum E_D = E_l + E_{sc} + E_f, \quad (7)$$

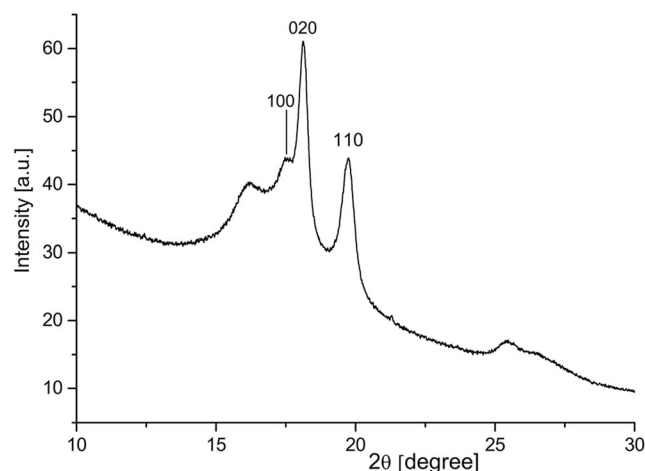


**Fig. 6** X-ray diffraction pattern for sample II



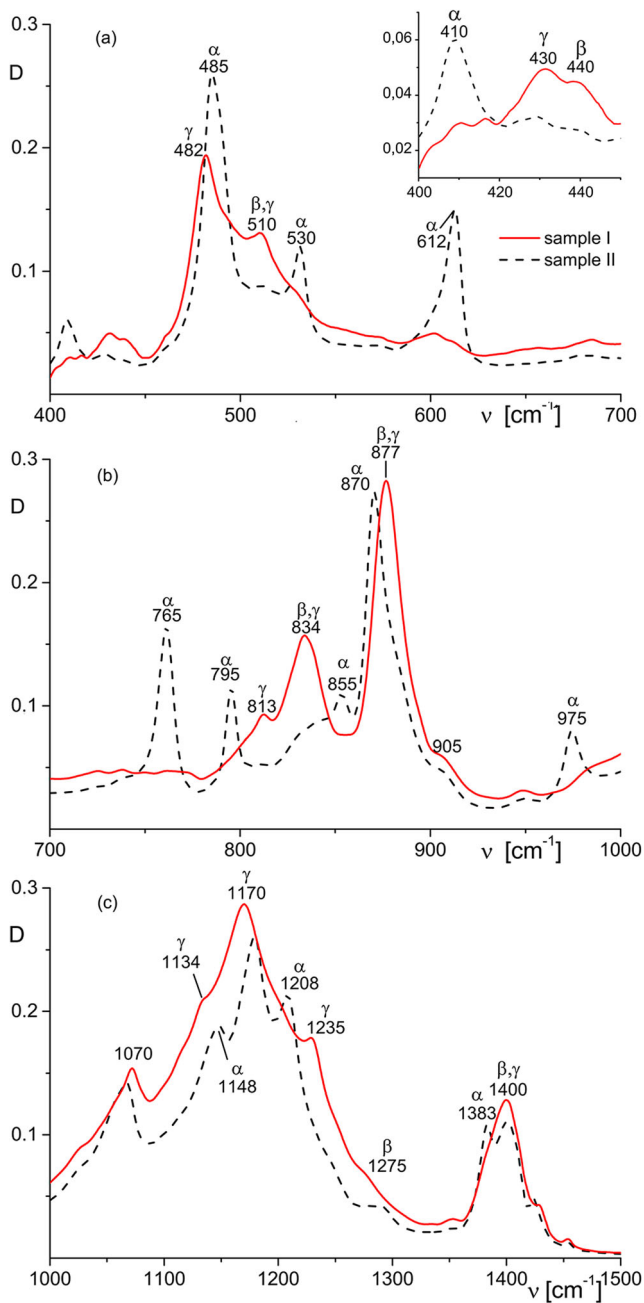


**Fig. 7** IR spectra of the copolymer films in the ranges of 400–700 (a), 700–1000 (b), and 1000–1500 (c)  $\text{cm}^{-1}$

where  $E_l$  is the component of the local field, which takes into account the linear contribution of the considered dielectric. If the polymer contains polar crystals (domains) in the bulk, then their contribution to the local field will be  $E_f$ . As noted above, the studied polymers are heterogeneous, and the crystalline and amorphous phases differ in conductivity and in permittivity. This creates a precondition for the appearance of Maxwell-Wagner polarization. It was observed, for example, in PVDF [16, 22], VDF/TFE [23], and in VDF/HFP copolymers [24]. The space charge with bulk density  $\rho(x, t)$  formed in the bulk of the film will also participate in the formation of the local field:

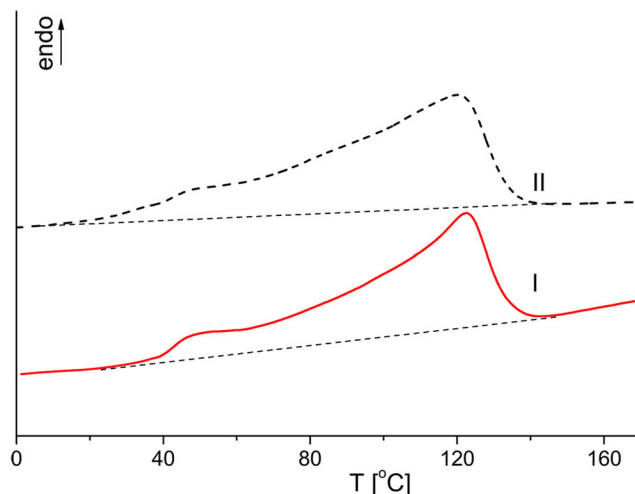


**Fig. 8** DSC thermograms of samples I and II at melting

$$E_{sc}(x, t) = \int_0^d \frac{\rho(x, t)}{\varepsilon_0 \varepsilon} dx \Big|_0^\infty dt, \quad 0 \leq x \leq d \quad (8)$$

If the crystallization proceeds with formation of polar crystals, then the fluctuating chains of the amorphous phase, which have increased free volume, may form anisotropic regions near the polar planes of the crystals (Fig. 9). This means that the field  $E_f$  contributes to the local field, which determines the molecular mobility of the chains in the amorphous phase. We can assume that  $E_f$  is equal to the depolarization field  $E_{dep}$  of the polar crystal. In this case, we write

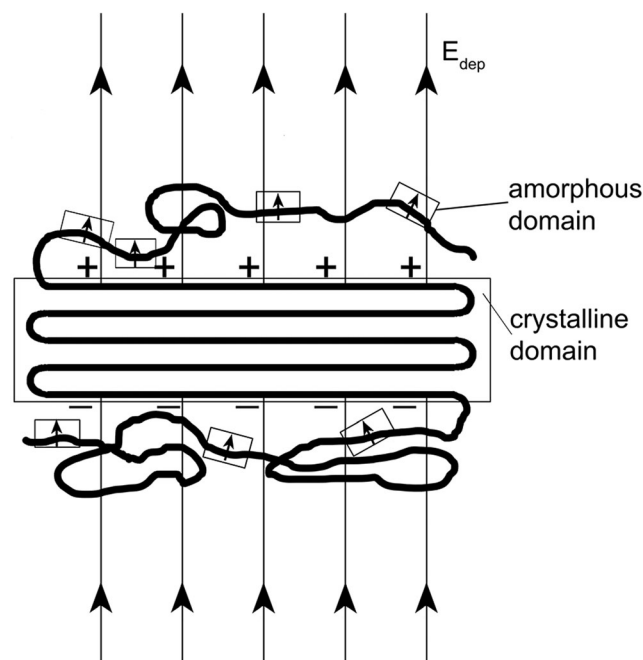


**Fig. 9** The model of polar PVDF crystal in the conformation of planar zigzag with formation of a certain long-range order in adjacent chains of the amorphous phase

$$E_f = E_{dep} = \frac{P}{\varepsilon_0 \varepsilon_f}, \quad (9)$$

where  $P$  is the polarization of ferroelectric crystal with dielectric permittivity  $\varepsilon_f$ . If we assume that for the perfect  $\beta$ -crystal  $P = 0.13 \text{ C/m}^2$  [1, 2], then it follows from Eq. (9) that near the polar planes of the crystals with  $\varepsilon_f = 5$ , the field  $E_f \sim 3 \text{ GV/m}$ .

All of the above means that the local field, which determines the relaxation of the chains in the amorphous phase above the glass transition temperature, is different in samples I and II. Indeed, in sample I, where the film crystallizes in the mixture of  $\beta$ - and  $\gamma$ -phases,  $E_f \neq 0$ , since the both phases have polar unit cells [1, 2, 10]. In contrast, in sample II  $E_f = 0$ , since the crystallization occurs in the centrosymmetric  $\alpha$ -phase, where the unit cell has a zero dipole moment [1, 2, 10]. In light of what has been said, it can be argued that the more intense temperature growth of  $\Delta\varepsilon$  for sample I should be related to the contribution of the field of the polar domains  $E_f$  to the resulting local field. As noted above,  $E_f$  reaches very high values near the surface of the polar crystal. Above the glass transition point, the amorphous phase is characterized by the increased free volume, and therefore the high dipole moment of its chains due to the orientation polarization can acquire a predominant direction due to the interaction with  $E_f$  (Fig. 9). The appearance of the local areas with a certain long-range order like in the nematic liquid crystal must lead to the decrease of the entropy of the system down to the value  $S_0$ . In this case, under the application of the external electric field  $E$ , the entropy of the dielectric will change to the value  $S$  [19].

$$S = S_0 + \frac{\partial \varepsilon_s}{\partial T} \frac{E^2}{8\pi} \quad (10)$$

As seen, if the derivative  $\frac{\partial \varepsilon_s}{\partial T}$  is positive, then the entropy in the field  $E$  will increase. It is possible only if before the application of the field the dipoles in the amorphous phase had some long-range order [19] that reduced the entropy of the system. As follows from Fig. 3 and from the inset in Fig. 5,  $\varepsilon_s$  increases with temperature. As seen from Table 1, the derivative is three times higher for the sample with polar crystals than for the sample crystallized predominantly in the non-polar  $\alpha$ -phase. It can be assumed that in the latter case, the less pronounced long-range order in the amorphous phase is due to the field of the space charges and to the presence of a small amount of  $\gamma$ -phase crystals. This can be seen from the presence of the weak absorption bands  $430, 510, 813, \text{ and } 840 \text{ cm}^{-1}$  typical for the  $T_3GT_3G^-$  conformation [1, 2, 10] in sample II.

If part of the chains of the amorphous phase (near the surfaces of polar crystals) in the polymers under consideration has a long-range order, then the thermal effect should be observed when this order is destroyed. We believe that the DSC data indicate this. As follows from Fig. 7, a weak endothermic

process is seen in both samples in addition to the main broad melting peak in the region of  $\sim 50^\circ\text{C}$ . In our opinion, this process is responsible for the destruction of the marked long-range order. As noted above, this order is more pronounced in sample I, and therefore, the thermal effect for the marked process should be higher. Indeed, it follows from our data (see Table 1), taking into account the selected method of drawing of the baseline for the low-temperature (lt) endothermic process. If the structuring effect for the chains of the amorphous phase near the crystal surfaces occurs in the polymers under consideration, then it should be observed both in PVDF itself and in its other copolymers. It follows from our previous papers [22–25] and from the papers of other authors [13–16], that in all these objects, the  $\alpha_a$ -relaxation is characterized by an increase in the relaxation strength with temperature. At the same time, according to our DSC data [22–25], the low-temperature endotherm is observed in all of the studied copolymers, which is associated with the destruction of the long-range order in the structured regions of the amorphous phase. It also can be seen on the example of VDF/TFE 94/6 copolymer (Fig. 10). The original film of the copolymer (heating 1), as in our case, was crystallized in a mixture of  $\beta$ - and  $\gamma$ -phases with polar crystals (Fig. 10). As seen from the inset to the figure, a weak endothermic process is noted for the initial film. After the crystallization from the melt at atmospheric pressure, this process disappears. IR spectroscopy data (Fig. 10, heating 2) shows that at this method of crystallization, non-polar  $\alpha$ -phase crystals begin to form, which, as mentioned above, do not create a local electric field. Thus, these data qualitatively coincide with the results obtained on the studied copolymers and confirm the hypothesis about the structuring of part of the chains of the amorphous phase near the polar planes of the ferroelectric domains.

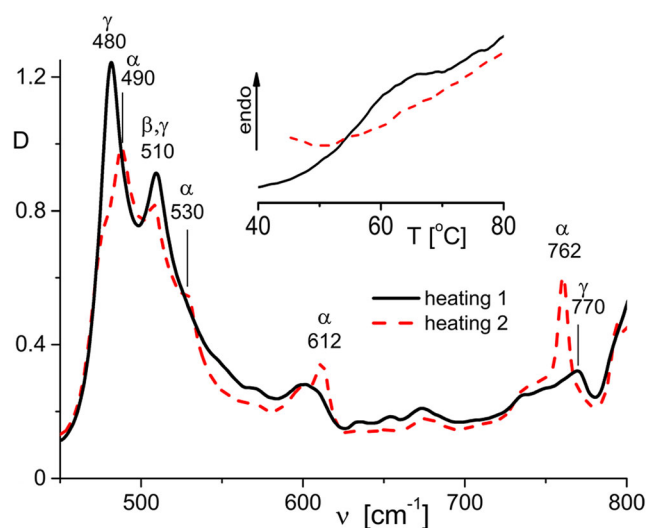


**Fig. 10** IR spectra and DSC thermograms (in the inset) of the VDF/TFE 94/6 copolymer films in initial state (heating 1) and after the crystallization from the melt at atmospheric pressure (heating 2) [25]

## Conclusion

Under certain conditions, the crystallization of the ferroelectric copolymer from a solution leads to the formation of the polar crystals. The local electric field near them is very high. A part of the chains of the amorphous phase near the polar planes of such crystals under the action of the noted field can form regions with a certain long-range order. The verification of this hypothesis was carried out by the analysis of the parameters of the dielectric dispersion in the region of cooperative mobility above the glass transition temperature. The temperature dependences of the static permittivity in two samples prepared under different crystallization conditions confirm this hypothesis. Indeed, in the case of the formation of the polar crystals, near which an enormously high local electric field can be detected, an indication on the formation of a fluctuating long-range order in the amorphous phase was found. Its destruction at temperature increase was registered by DSC.

**Acknowledgments** The authors would like to thank V.S. Khurdin for the help in the measurements and data analysis.

**Funding information**

The work was supported by the Russian Foundation for Basic Research (RFBR 18-03-00493).

## Compliance with ethical standards

**Conflicts of interest** The authors declare that they have no conflict of interest.

**Publisher's note** Springer Nature remains neutral with regard to jurisdictional claims in published maps and institutional affiliations.

## References

- Wang TT, Herbert JM, Glass AM (eds) (1988) The application of ferroelectric polymers. Blackie, Glasgow
- Nalva HS (ed) (1995) Ferroelectric polymers—chemistry, physics and applications. Marcel Dekker Inc, New York
- Kochervinskii VV (1994) The properties and applications of fluorine-containing polymer films with piezo- and pyro-activity. *Russ Chem Rev* 63(4):367–371. <https://doi.org/10.1070/RC1994v063n04ABEH000090>
- Granz B (1989) PVDF hydrophone for the measurement of shock waves (lithotripsy). *IEEE Trans Electr Insul* 24(3):499–502. <https://doi.org/10.1109/14.30896>
- Hughes WJ (1992) Underwater polyvinylidene fluoride PVDF acoustic sensors. *J Acoust Soc Am* 91:2335. <https://doi.org/10.1121/1.403503>
- Markose S, Patange SR, Raja S, Jain A, Elias B (2013) Experimental study on dimension effect of PVDF film on energy harvesting. *Int J Adv Res Electrical Electron Instrum Eng* 2:270–278
- Latour M, Murphy PV (1981) Application of PVF<sub>2</sub> transducers as piezoelectric vibrators for marine fouling prevention. *Ferroelectrics* 32(1):33–37. <https://doi.org/10.1080/00150198108238670>
- Neese B, Chu B, Lu S-G, Wang Y, Furman E, Zhang QM (2008) Large electrocaloric effect in ferroelectric polymers near room temperature. *Science* 321(5890):821–823. <https://doi.org/10.1126/science.1159655>
- Zhou X, Zhao X, Suo Z, Zou C, Runt J, Liu S, Zhang S, Zhang QM (2009) Electrical breakdown and ultrahigh electrical energy density in poly(vinylidene fluoride-hexafluoropropylene) copolymer. *Appl Phys Lett* 94(162901):5–3. <https://doi.org/10.1063/1.3123001>
- Kochervinskii VV (1996) The structure and properties of block poly(vinylidene fluoride) and systems based on it. *Russ Chem Rev* 65(10):865–913. <https://doi.org/10.1070/RC1996v065n10ABEH000328>
- Vogel H (1921) The law of relation between the viscosity of liquids and the temperature. *J Amer Ceram Soc* 8:339–355
- Kochervinskii VV, Kiselev DA, Malinkovich MD, Pavlov AS, Malyshkina IA (2015) Local piezoelectric response, structural and dynamic properties of ferroelectric copolymers of vinylidene fluoride–tetrafluoroethylene. *Colloid Polym Sci* 293:533–543. <https://doi.org/10.1007/s00396-014-3435-1>
- Sasabe H, Saito S, Asahina M, Kakutani H (1969) Dielectric relaxations in poly(vinylidene fluoride). *J Polym Sci A-2* 7(8):1405–1414. <https://doi.org/10.1002/pol.1969.160070810>
- Koizumi N, Yano S, Tsunashima K (1969) Dielectric relaxation of poly(vinylidene fluoride). *J Polym Sci C* 7(1):59–64. <https://doi.org/10.1002/pol.1969.110070113>
- Nakagawa K, Ishida Y (1973) Dielectric relaxations and molecular motions in poly(vinylidene fluoride) with crystal form II. *J Polym Sci Polym Phys Ed* 11:1503–1533. <https://doi.org/10.1002/pol.1973.180110804>
- Yano S, Tadano K, Aoki K, Koizumi N (1974) Alternating-current ionic conduction and dielectric relaxation of poly(vinylidene fluoride) at high temperatures. *J Polym Sci B Polym Phys* 12:1875–1887. <https://doi.org/10.1002/pol.1974.180120911>
- Miyamoto Y, Miyaji H, Asai K (1980) Anisotropy of dielectric relaxation in crystal form II of poly(vinylidene fluoride). *J Polym Science: Polym Phys Ed* 18:597–606. <https://doi.org/10.1002/pol.1980.180180318>
- Böhmer R, Ngai KL, Angell CA, Plazek DJ (1993) Nonexponential relaxations in strong and fragile glass formers. *J Chem Phys* 99:4201–4209. <https://doi.org/10.1063/1.466117>
- Frohlich H (1958) Theory of dielectrics: dielectric constant and dielectric loss. Clarendon Press, Oxford
- Kremer F, Schonhals A (eds) (2003) Broadband dielectric spectroscopy. Springer-Verlag, Berlin Heidelberg
- Blythe AR, Bloor D (2005) Electrical properties of polymers. Cambridge University Press, New York
- Kochervinskii V, Malyshkina I, Gavrilova N, Sulyanov S, Bessonova N (2007) Peculiarities of dielectric relaxation in poly(vinylidene fluoride) with different thermal history. *J Non-Cryst Sol* 353:4443–4447. <https://doi.org/10.1016/j.jnoncrsol.2007.03.034>
- Kochervinskii VV, Malyshkina IA, Pavlov AS, Pakuro NI, Bessonova NP, Shmakova NA, Bedin SA, Chubunova EV, Lebedinskii YY (2015) An effect of the electrode material on space charge relaxation in ferroelectric copolymers of vinylidene fluoride. *J Appl Phys* 118(24):244102 (1–9). <https://doi.org/10.1063/1.4938016>
- Kochervinskii VV, Malyshkina IA, Markin GV, Gavrilova ND, Bessonova NP (2007) Dielectric relaxation in vinylidene fluoride-hexafluoropropylene copolymers. *J Appl Polym Sci* 105:1101–1117. <https://doi.org/10.1002/app.26145>
- Kochervinskii V, Kozlova N, Malyshkina I, Astakhov V (2018) Structural aspects of the high-temperature space charge relaxation in ferroelectric VDF/TFE 94/6 copolymer. *Ferroelectrics* 531:1–21. <https://doi.org/10.1080/00150193.2018.1497407>